Heliyon 9 (2023) e19034

Contents lists available at ScienceDirect

Heliyon

journal homepage: www.cell.com/heliyon

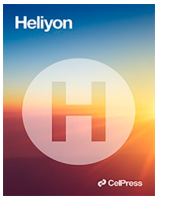

Long noncoding RNA HOXC-AS3 remodels lipid metabolism and promotes the proliferation of transformed macrophages in the glioma stem cell microenvironment by regulating the hnRNPA1/CaM axis

Yujing Sheng [a,1], Baomin Chen [a,1], Liang Liu [b,1], Suwen Li [a], Shilu Huang [a], Shan Cheng [a], Zhe Li [c,**], Yifang Ping [d], Zhigang Gong [e], Jun Dong [a,*]

[a] Department of Neurosurgery, Second Affiliated Hospital of Soochow University, Suzhou, China
[b] Department of Neurosurgery, Affiliated Nanjing Brain Hospital, Nanjing Medical University, Nanjing, Jiangsu, China
[c] State Key Laboratory of Analytical Chemistry for Life Science, Nanjing University, Nanjing, China
[d] Institute of Pathology and Southwest Cancer Center, Southwest Hospital, Third Military Medical University, Chongqing, China
[e] Department of Neurosurgery, Suzhou TCM Hospital Affiliated of Nanjing University of Chinese Medicine, Suzhou, China

ARTICLE INFO

Keywords:
Glioma stem cells
Transformed macrophages
Lipid metabolism remodelling
HOXC-AS3
Tumour microenvironment

ABSTRACT

Metabolism remodelling of macrophages in the glioblastoma microenvironment contributes to immunotherapeutic resistance. However, glioma stem cell (GSC)-initiated lipid metabolism remodelling of transformed macrophages (tMΦs) and its effect on the glioblastoma microenvironment have not been fully elucidated. Total cholesterol (TC) levels and lipid metabolism enzyme expression in macrophages in the GSC microenvironment were evaluated and found that the TC levels of tMΦs were increased, and the expression of the lipid metabolism enzymes calmodulin (CaM), apolipoprotein E (ApoE), and liver X receptor (LXR) was upregulated. Knockdown of HOXC-AS3 led to a decrease in the proliferation, colony formation, invasiveness, and tumorigenicity of tMΦs. Downregulation of CaM resulted in a decline in TC levels. HOXC-AS3 overexpression led to increases in both CaM expression levels and TC levels in tMΦs. RNA pull down and mass spectrometry experiments were conducted and heterogeneous nuclear ribonucleoprotein A1 (hnRNPA1) was screened as the HOXC-AS3 binding proteins related to lipid metabolism. RIP and RNA pull down assays verified that HOXC-AS3 can form a complex with hnRNPA1. Knockdown of hnRNPA1 downregulated CaM expression; however, downregulation of HOXC-AS3 did not affect hnRNPA1 expression.TMΦs underwent lipid metabolism remodelling induced by GSC via the HOXC-AS3/hnRNPA1/CaM pathway, which enhanced the protumor activities of tMΦs, and may serve as a potential metabolic intervening target to improve glioblastoma immunotherapy.

* Corresponding author.
** Corresponding author.
E-mail addresses: zheli@nju.edu.cn (Z. Li), dongjun@suda.edu.cn (J. Dong).
[1] These authors contributed equally to this work and share first authorship.

https://doi.org/10.1016/j.heliyon.2023.e19034
Received 16 April 2023; Received in revised form 31 July 2023; Accepted 3 August 2023
Available online 9 August 2023

1. Introduction

The prognosis of glioblastoma multiforme (GBM) patients is very poor, and the median overall survival is less than 15 months, even after active comprehensive treatment due to the high proliferation, high heterogeneity, high invasiveness, high therapeutic resistance, and high recurrence of GBM [1,2]. The abovementioned "5H" biological characteristics of GBM are a result of glioma stem cell (GSC)-induced tissue remodelling, which includes the transformation of various kinds of interstitial cells in the GBM microenvironment (GME). These transformed interstitial cells contribute to high heterogeneity and high therapeutic resistance via metabolism remodelling [3–6]. However, the potential mechanism of metabolic remodelling of these transformed interstitial cells in the GSC-remodelled microenvironment has not been completely clarified.

Tumour-associated macrophages (TAM) are abundant in the GME and play vital roles in promoting both tumour progression and immunotherapy resistance [7–9]. TAM significantly contribute to the construction of a highly immunosuppressive GME dominated by GSC [10]. Recently, the molecular mechanism by which macrophage transform into TAM within the protumor GBM immune microenvironment (GIME) stimulated by GSC has been widely investigated [11,12].

Our recent studies further revealed that the macrophages (MΦ) transformed into TAM in the GSC-remodelled GIME after mutual interactions with GSC, and that transformed macrophages (tMΦs) highly expressed the M2 macrophage markers Arg-1, FIZZ1 and CD163, and exhibited enhanced glucose metabolism [13–15]. Moreover, targeting the miR-449/MCT1 axis significantly inhibited glucose metabolism in tMΦs and decreased the proliferation and invasiveness of tMΦs [16]. Lipid metabolism remodelling of TAM has been reported in several noncentral nervous system malignancies [17,18]; however, lipid metabolism remodelling of tMΦs in the GIME has not been fully elucidated.

Long noncoding RNA (lncRNA) are noncoding RNA molecules of greater than 200 nucleotides in length that act as molecular sponges and interact with proteins, mRNAs, and miRNAs, thereby regulating the expression of target genes [19]. Previous studies have reported that HOXC-AS3 is associated with the progression of various cancers, such as ovarian cancer [20] and breast cancer [21]. In GBM, the homeotic box family gene HOXB13 promoted the proliferation, migration and invasiveness of tumour cells through transcriptional upregulation of HOXC-AS3 [22]. Another study reported that HOXC-AS3 promoted glioma progression by activating miR-216, which regulated F11R expression [23]. However, the potential mechanism by which HOXC-AS3 regulates the lipid metabolism of macrophages in the GIME has not been reported previously. In this study, we explored the roles of HOXC-AS3 in inhibiting both aberrant lipid metabolism and tMΦs proliferation and investigated whether HOXC-AS3 promoted cell proliferation and invasiveness of tMΦs by regulating their lipid metabolism remodelling.

2. Materials and methods

2.1. Cell lines and cell culture

TMΦs (including $tM\Phi_1$ and $tM\Phi_2$ cells) were cloned from in vivo and in vitro GSC and MΦ mutual interaction models generated in our previous studies [13–15]. These cells were cultured in Dulbecco's modified Eagle's medium (DMEM, Gibco, NY, USA) supplemented with 10% foetal bovine serum (FBS, ScienCell, LA, USA) in an incubator (ESPEC BNA-311, Japan) with 5% CO_2 at 37 °C. Primary culture of naive macrophages was achieved by collecting murine bone marrow stem cells and inducing them to differentiate into MΦ in α-MEM containing 5 ng/ml M-CSF (MCE, NJ, USA) with 10% FBS according to the previous studies [24].

2.2. Intracellular total cholesterol measurement

Intracellular total cholesterol (TC) levels were measured using a total cholesterol assay kit (Solarbio, Beijing, China) according to the manufacturer's instructions. Briefly, a total of 5×10^6 cells in the logarithmic growth phase were collected after centrifugation, 1 ml of cell lysis buffer (Reagent I) was added to the cell pellet, and then ultrasonication was performed (power 300 W, ultrasonic emission 2 s, stop 3 s, repeated 30 times). After centrifugation at 10000×*g* for 10 min at 4 °C, the supernatant was collected, and 180 μl working solution was added to 20 μl supernatant samples and then incubated at 37 °C for 15 min. The OD value at 500 nm was measured with a multimode plate reader (TECAN Infinite 200 Pro, Switzerland) to quantify intracellular TC levels.

Table 1
The primer sequences used in the present study.

Gene	Primer sequences
HOXC-AS3	Forward primer: 5′-GTGGAGTAACAGCGCCATCT-3′
	Reverse primer: 5′-CGGGTTTTGTTGCGTCTTGT-3′
CaM	Forward primer: 5′-ATGTCGGATTTTGACAGCAACC-3′
	Reverse primer: 5′-GTCCCGGTGGCACATTTCT-3′
hnRNPA1	Forward primer: 5′-ATGTCTAAGTCCGAGTCTCCCA-3′
	Reverse primer: 5′-TGTTAGTGTTCCCCATTGCTC-3′
β-actin	Forward primer: 5′-CGTTGACATCCGTAAAGACC-3 ′
	Reverse primer: 5′-AACAGTCCGAGAAGCAC-3 ′
U6	Forward primer: 5′-CTCGCTTCGGCAGCACA-3′
	Reverse primer: 5′-AACGCTTCACGAATTTGCGT-3′

2.3. Real-time quantitative PCR

Total RNA was isolated with TRIzol (Invitrogen, Carlsbad, CA, USA) and reverse transcribed into cDNA using Fermentas reverse transcription reagent (Applied Biosystems, Thermo Fisher Scientific, MA, USA). Then, real-time quantitative PCR (qRT−PCR) was conducted with SYBR Green PCR Master Mix (Applied Biosystems, Thermo Fisher Scientific, MA, USA) according to the manufacturer's protocols via the $2^{-\triangle\triangle Ct}$ method. The primer sequences used in the present study are listed in Table 1.

2.4. Western blot

Total cellular proteins were extracted with RIPA lysis buffer (Beyotime, Shanghai, China) and quantified with a BCA protein assay kit (Beyotime, Shanghai, China) according to the manufacturer's protocol. Next, 10 μg of total proteins were separated under electrophoresis in 10% SDS−PAGE and transferred to PVDF membrane (Millipore, Bedford, MA, USA), followed by blocking with 5% skimmed milk for 2 h at room temperature. The membrane was incubated with primary antibodies (anti-CaM, ApoE, LXR or hnRNPA1, diluted 1:1000, Abcam, Cambridge, MA, USA) overnight at 4 °C, washed three times with PBS and incubated with horseradish peroxidase (HRP)-labelled secondary antibody (diluted 1:10000, CST, MA, USA) for 1 h at room temperature. β-actin (1:1000, Bioss, Beijing, China) was used as a control gene. Finally, the bands were visualized and recorded with Image Quant LAS 4000 mini (GE Healthcare, USA).

2.5. Expression vector construction and cell transfection

A lentiviral vector was used to construct HOXC-AS3 overexpression and HOXC-AS3 knockdown vectors. Both overexpression vector and lentiviral particles were synthesized by GenePharma, Shanghai, China. Briefly, single cell suspensions (5×10^5 cells/ml) of $tM\Phi_1$ of $tM\Phi_2$ were prepared and inoculated in 6-well plates (2 ml/well.) HOXC-AS3 group were tMΦ cell lines transfected with HOXC-AS3 overexpression plasmid as the experimental groups, and the corresponding empty transfection group (NC group) was the control group. shHOXC-AS3 group were transfected with HOXC-AS3 RNAi lentivirus, and the corresponding empty transfection group (sh-NC group) was the control group. After 24 h of transfection, the culture medium was replaced with fresh medium containing HBLV-U6 lentiviral vector (Hanbio, Shanghai, China), and polyclathrin ((Hanbio, Shanghai, China, final concentration 5 μg/ml) was added. After 18 h of infection (according to the pre-experimental optimization), the medium was changed to conventional medium and the cells were screened by adding puromycin (MCE, NJ, USA, final concentration 5 μg/ml) to observe cell growth and verify the infection efficiency by qRT-PCR.

2.6. Cell proliferation evaluation

A CCK-8 (Beyotime, Shanghai, China) assay was performed according to the manufacturer's protocol. Cells were seeded into 96-well plates in 100 μl of culture media. The medium of each well was replaced with 100 μl of fresh culture media with 10% CCK-8 reagent at different times (1, 2, 3, and 4 d), and then the cells were incubated for an additional 3 h. The absorbance was measured at an optical density of 450 nm using a microplate reader (Tecan Infinite 200 PRO, Switzerland).

2.7. Clone formation assay

Cells were seeded at a density of 100 cells/well in a culture dish (60 mm, Corning, NY, USA) and cultured at 37 °C with 5% CO_2. Twelve days later, the cells were fixed with paraformaldehyde for 5 min and then stained with crystal violet for 20 min.

2.8. Invasiveness assay

Chamber inserts (Merck Millipore, Germany) were precoated with 45 μL Matrigel (1:8 dilution; BD Bioscience, NJ, USA). A total of 5×10^4 cells in serum-free medium were seeded into the upper chamber, and DMEM containing 10% FBS was added to the lower chamber. After incubation for 48 h at 37 °C with 5% CO_2, the lower chamber was fixed with 4% paraformaldehyde for 5 min, stained with crystal violet solution for 30 min, washed 3 times with PBS (Gibco, NY, USA), and then observed and counted under a microscope.

2.9. Tumour xenograft model

Female BALB/c athymic nude mice were housed on sterile bedding in microisolator cages (NASA1000) with water and food provided ad libitum. All animal studies were approved by the Ethics Committee of Soochow University (Approval No. SUDA20210708A03) and conducted in facilities that were approved by the Chinese Experimental Animal Association. Briefly, tMΦs transfected with sh-RNA targeting HOXC-AS3 or control vector (5×10^6/0.5 ml) were injected subcutaneously (s.c.) in the right axillary region of mice at 6–8 weeks of age with an approximate body weight of 20 g. The subcutaneous tumours were measured in two dimensions with a calliper two times a week. Tumour size was calculated using the formula ($a^2 \times b$)/2 (a: width in mm, b: length in mm) and can be converted to weight from unit density (i.e., 1 $mm^3 = 1$ mg). After 30 days, all mice were sacrificed general anaesthesia, and tumour weight and volume were measured.

2.10. RNA pull-down and mass spectrometry

One microgram of labelled lncRNA HOXC-AS3 in RNA structure buffer containing 10 mmol/L Tris (pH = 7), 0.1 mol/L KCl, and 10 mmol/L $MgCl_2$ was heated to 95 °C for 2 min. Then, the labelled RNA was incubated on ice for 3 min, followed by incubation at room temperature for 30 min to allow RNA to form a suitable secondary structure. The beads were washed with washing buffer and added to the RNA sample with secondary structure overnight at 4 °C. After centrifugation at 3000×*g* for 1 min, the supernatant was discarded, the beads were washed with washing buffer 3 times, and then the cell lysate was added for 1 h at room temperature. The magnetic bead-RNA−protein mixture was centrifuged at low speed, the supernatant was collected, 5 × SDS sample buffer was added, and the mixture was kept at 95 °C for 10 min for degeneration. The proteins were separated by SDS−PAGE, stained with Coomassie brilliant blue, and fragmented into the target band for mass spectrometry. Hystar software was used to adjust the instrument parameters to obtain appropriate mass spectrometry data. HOXC-AS3 binding proteins associated with lipid metabolism were screened out from the highly enriched proteins.

2.11. RNA immunoprecipitation (RIP)

A total of 5×10^6 $tM\Phi_1$ or $tM\Phi_2$ cells were harvested, and immunoprecipitation lysis buffer was added for 30 min at 4 °C and then centrifuged at 12,000×*g* for 30 min to remove the supernatant. The lysate pellet was fully dissolved with 1 μg hnRNPA1 antibody and 50 μl protein A/G-beads and incubated overnight at 4 °C. After centrifugation at 3000×*g* for 5 min at 4 °C, the supernatant was removed, and the protein A/G-beads were washed three times with 1 ml lysis buffer. Then, 15 μL 2 × SDS sample buffer was added, and the beads were soaked in boiling water for 10 min qRT−PCR analysis was performed to quantify the amount of HOXC-AS3 binding with hnRNPA1.

2.12. Statistical analysis

All experiments were repeated three times independently. SPSS 13.0 software was used for statistical data analysis. All data are expressed as the mean ± standard error. A non-parametric *t*-test (two groups) or one-way ANOVA (three groups or more) was applied to analyse the statistical significance. A *P value* of less than 0.05 was considered statistically significant.

3. Results

3.1. Transformation of macrophages in the GSC-remodelled microenvironment

Interactions between naive macrophages and GSC were observed in vitro and invivo, and macrophages malignantly transformed. Namely, naive macrophages acquired unlimited proliferation potential and high tumorigenicity while still retaining the MΦ surface markers CD68 and F4/80. These results were consistent with our previous findings [13,14].

3.2. Lipid metabolism remodelling of tMΦs

The level of intracellular total cholesterol in $tM\Phi_1$ and $tM\Phi_2$ cells was significantly higher than that in naive MΦs (Fig. 1A). The protein expression levels of calmodulin (CaM), apolipoprotein E (ApoE), and liver X receptor (LXR), which are related to cholesterol synthesis, storage and transportation, respectively, in $tM\Phi_1$ and $tM\Phi_2$ cells were all higher than those in naive MΦs (Fig. 1B and C and Supplementary Fig.S1). CaM expression was the most significantly upregulated in tMΦs.

3.3. HOXC-AS3 knockdown significantly inhibited the proliferation, invasiveness and tumorigenicity of tMΦs

QRT-RCR was performed to verified the transfection efficiency based on the lentivirus vector (Supplementary Fig. S2). HOXC-AS3

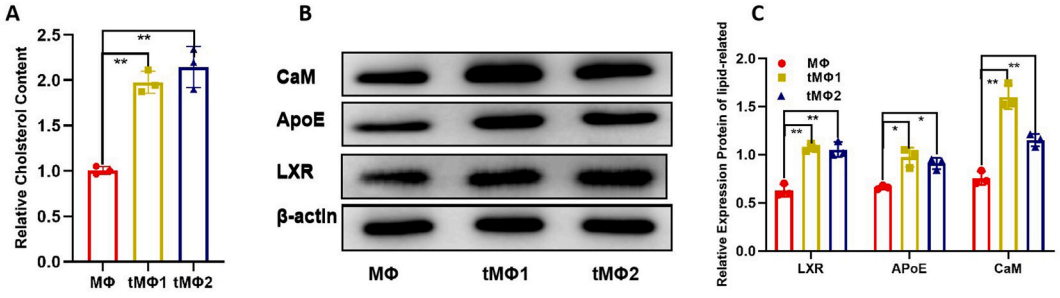

Fig. 1. The lipid metabolism characteristics of transformed macrophages. **A** The intracellular TC level in $tM\Phi_1$ and $tM\Phi_2$ cells was higher than that in naive MΦs. **B, C** The protein levels of CaM, ApoE and LXR obviously increased in $tM\Phi_1$ and $tM\Phi_2$ cells, compared with naive MΦs. (**$P < 0.001$).

expression in tMΦ$_1$ and tMΦ$_2$ cells was significantly higher than that in naive MΦs in the GSC microenvironment (Fig. 2A). Downregulation of HOXC-AS3 expression resulted in inhibition of cell proliferation and invasiveness of transformed MΦs both in vitro and in vivo. Specifically, CCK-8 and clone formation assays results showed downregulation of HOXC-AS3 inhibited cell proliferation ability and decreased clone formation number of tMΦ$_1$ and tMΦ$_2$ cells (Fig. 2B–D), and an invasiveness assay showed that the number of migratory cells decreased as well (Fig. 2E and F). Knockdown of HOXC-AS3 also led to slowed tMΦ$_1$ cell growth in vivo (Fig. 2G and H). These data suggest that HOXC-AS3 plays an active role in promoting the malignant phenotype in tMΦs.

3.4. HOXC-AS3 increased lipid metabolism in tMΦs by regulating CaM

To further explore the potential mechanism by which HOXC-AS3 increased both lipid metabolism and the cell proliferation ability

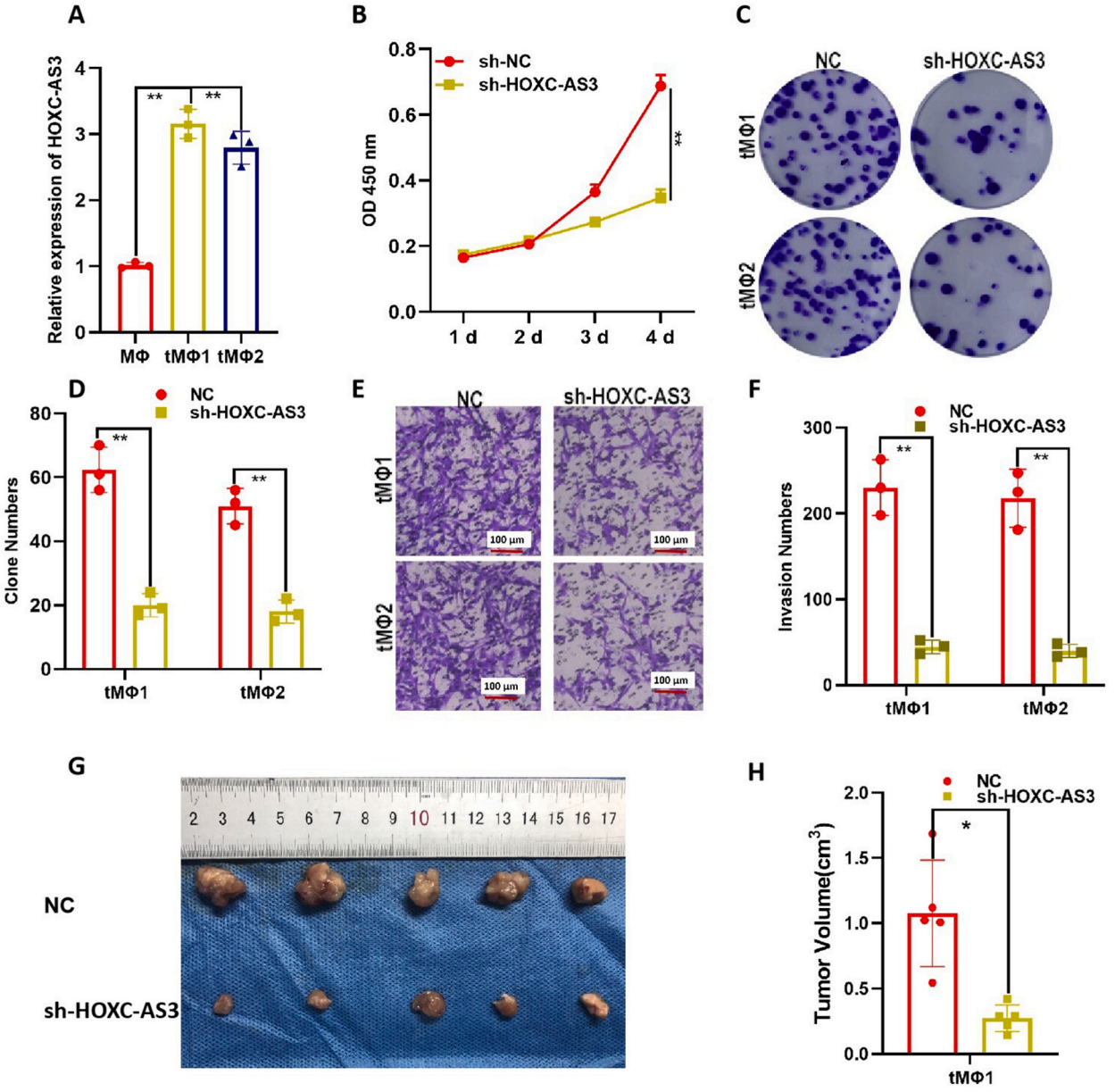

Fig. 2. HOXC-AS3 knockdown inhibited the proliferation, invasiveness and tumorigenicity of tMΦs. **A** qRT-PCR suggested that HOXC-AS3 expression in tMΦ$_1$ and tMΦ$_2$ cells was significantly higher than that in naive MΦs. **B** CCK-8 assay results showed downregulation HOXC-AS3 inhibited proliferation malignant in tMΦ$_1$ and tMΦ$_2$ cells. **C, D** Clone formation assay (magnification:200×) showed that cell clone numbers were decreased. **E, F** Invasiveness assay (magnification:200×) showed that the numbers of migratory cells decreased as well. **G, H** Knockdown of HOXC-AS3 also led to slowed tMΦ$_1$ cell growth in vivo. (*$P < 0.05$, **$P < 0.001$).

of tMΦs, as well as the regulatory relationship between HOXC-AS3 and CaM, qRT−PCR and Western blotting were performed. The results showed that CaM expression was downregulated after HOXC-AS3 knockdown and upregulated after HOXC-AS3 overexpression in both $tMΦ_1$ and $tMΦ_2$ cells (Fig. 3A–C and Supplementary Fig. S3). Intracellular TC levels in $tMΦ_1$ and $tMΦ_2$ cells clearly decreased after HOXC-AS3 downregulation and clearly increased after HOXC-AS3 overexpression (Fig. 3D). There was a positive correlation between the expression of HOXC-AS3 and CaM, which implied that HOXC-AS3 affected the lipid metabolism of tMΦs by regulating CaM expression.

In addition, the regulatory effect of HOXC-AS3 on other proteins related to lipid metabolism (ApoE and LXR) were also observed, and the overall positive regulatory effect was verified by qRT−PCR and Western blotting (Fig. 4 and Supplementary Fig. S4).

3.5. *HOXC-AS3 regulated CaM expression by binding hnRNPA1*

To reveal the potential mechanism by which HOXC-AS3 regulates CaM expression, proteomics analysis was performed, which showed that heterogeneous nuclear ribonucleoprotein A1 (hnRNPA1), a potential candidate protein, had the highest binding probability based on peptide sequence coverage of 42.18% in $tMΦ_1$ cells and 31.76% in $tMΦ_2$ cells. RNA pull-down and RIP assays showed that hnRNPA1 protein was pulled down by the HOXC-AS3 probe and that HOXC-AS3 was precipitated by the hnRNPA1 antibody in tMΦs. This result confirmed that hnRNPA1 can form a complex with HOXC-AS3 (Fig. 5A and B and Supplementary Fig. S5). Knockdown of hnRNPA1 downregulated CaM expression (Fig. 5C and Supplementary Fig. S6). The effect of hnRNPA1 knockdown on CaM was almost the same as that of HOXC-AS3 knockdown. In addition, obvious hnRNPA1 expression changes at the transcriptional or protein level could not be observed after HOXC-AS3 knockdown in both $tMΦ_1$ and $tMΦ_2$ cells (Fig. 5D and E and Supplementary Fig. S7), which implied that HOXC-AS3 can bind with hnRNPA1 because of their matched spatial structure and natural affinity. However, HOXC-AS3 did not degrade or promote hnRNPA1 transcription; hence, hnRNPA1 expression was independent of HOXC-AS3. HOXC-AS3 binding with hnRNPA1 reduced the probability of hnRNPA1 binding with CaM, thus producing a similar effect of CaM upregulation.

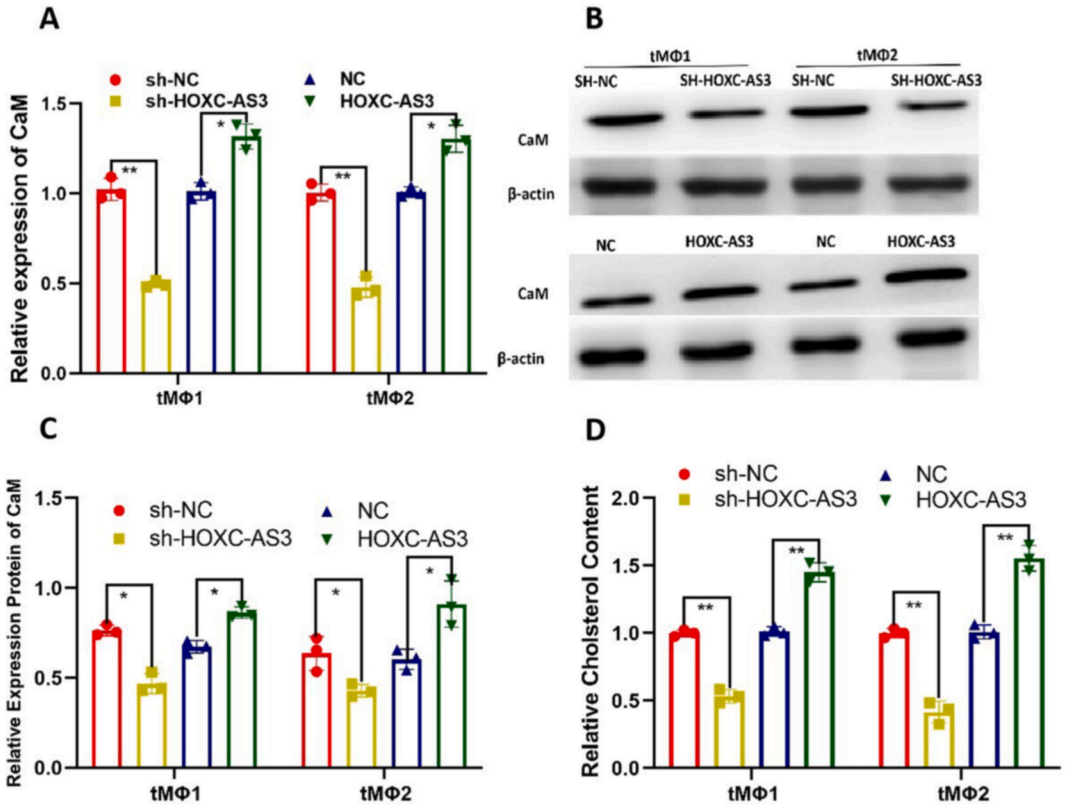

Fig. 3. CaM expression and intracellular TC levels of transformed macrophages was positively correlated with HOXC-AS3 level. **A-C** qRT-PCR and Western blotting showed that CaM expression was downregulated after HOXC-AS3 knockdown and upregulated after HOXC-AS3 overexpression in both $tMΦ_1$ and $tMΦ_2$ cells. **D** Intracellular TC levels in $tMΦ_1$ and $tMΦ_2$ cells clearly decreased after HOXC-AS3 downregulation and clearly increased after HOXC-AS3 overexpression. (*P < 0.05, **P < 0.001).

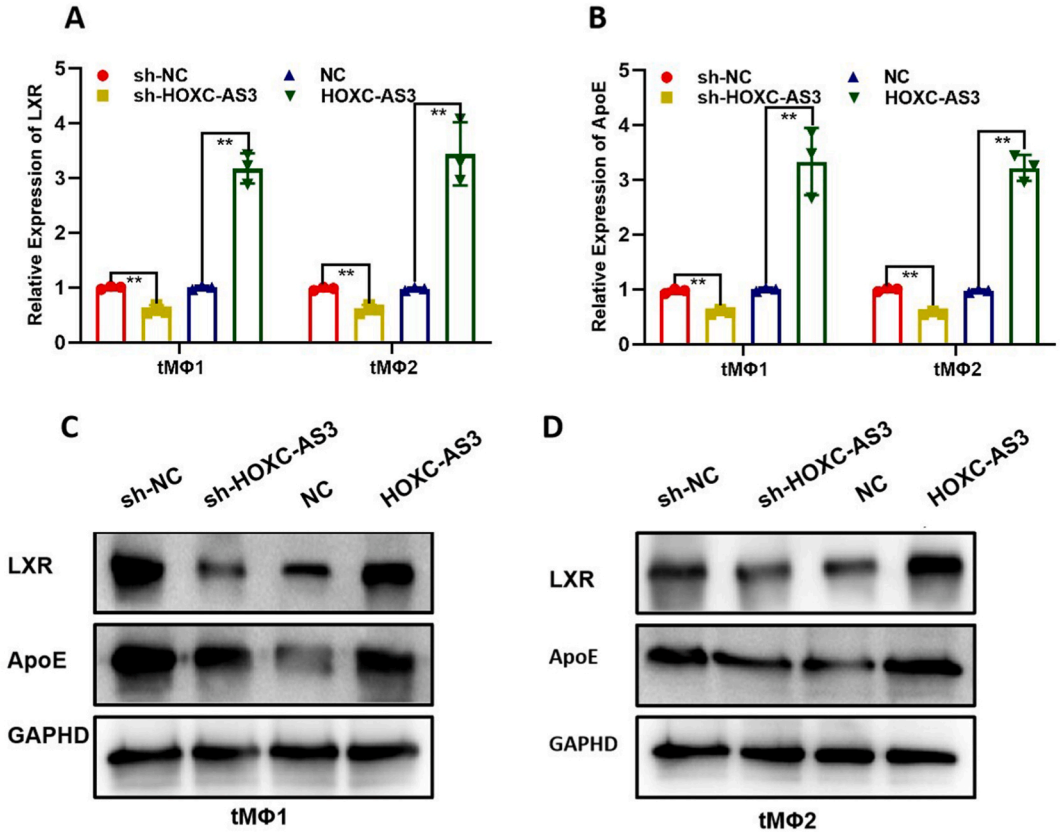

Fig. 4. LXR and ApoE expression was positively correlated with HOXC-AS3. qRT-PCR **(A, B)** and Western bolt **(C, D)** showed that LXR and ApoE expression was downrugulated after HOXC-AS3 knockdown and upregulated after HOXC-AS3 overexpression in both $tM\Phi_1$ and $tM\Phi_2$ cells. (**$P < 0.001$).

4. Discussion

Malignant transformation of macrophages in GSC-MΦ mutual interaction models has been observed in our previous studies [13,15], and aberrant glucose metabolism in tMΦs has been reported [16]. Recent investigations have revealed aberrant energy metabolism in GBM, especially the metabolic patterns of GSC and interstitial cells in the GSC-constructed microenvironment, which have all been remodelled to favour and support tumour development [25]. The metabolism phenotype with aberrant glycolysis has become one of the new malignant characteristics of gliomas [26]. Several studies have shown that TAM metabolism in the tumour microenvironment (TME) also undergoes metabolic remodelling with an enhanced glycolysis pathway [27,28]. However, lipid metabolism and its role in remodelling the functional metabolic phenotype of TAM when cross-talking with GSC has not been fully elucidated. In a lung carcinoma model, macrophages underwent metabolic changes, especially in their lipid profile, and the cell populations representing resident alveolar macrophages and TAM had different expression levels of multiple genes related to lipid metabolism signalling [29]. Goossens reported that ovarian cancer cells promoted the efflux of membrane cholesterol, which shifted TAM to the M2-like phenotype and promoted tumour progression [30]. Recent studies have shown that specific interventions in the lipid metabolism of immune cells in the TME can improve the efficacy of tumour immunotherapy. The LXR agonist GW3965 promoted ApoE production and reduced the formation of neovascularization in tumours, and phase I clinical trials showed that GW3965 treatment reduced the number of immunosuppressive cells, including TAM, and activated the antitumour immune response in lymphoma patients [31]. Another study found that intervention against the fatty acid metabolism of $CD8^+$ T cells in the TME improved the effect of immunotherapy against melanoma [32]. The abovementioned results suggest that precise intervention in lipid metabolism remodelling of transformed immune cells is a potential new strategy for GBM immunotherapy. Our results also showed that the intracellular TC level of tMΦs significantly increased, and the expression of CaM, ApoE and LXR was significantly upregulated, indicating that lipid metabolism in tMΦs was enhanced after crosstalk with GSC.

Downregulation of HOXC-AS3 in gliomas and its effect on inhibited tumour cell proliferation and invasiveness have been reported [22,23]. However, the potential mechanism by which HOXC-AS3 regulates lipid metabolism in tMΦs in the GIME has not been previously investigated. The current study indicated upregulation of HOXC-AS3 in tMΦs, and upregulated HOXC-AS3 expression further promoted the proliferation and invasiveness of tMΦs by regulating their lipid metabolism remodelling by the hnRNPA1/CaM pathway. CaM is a calcium binding protein that regulates the posttranscriptional modification of key transcription factors (such as

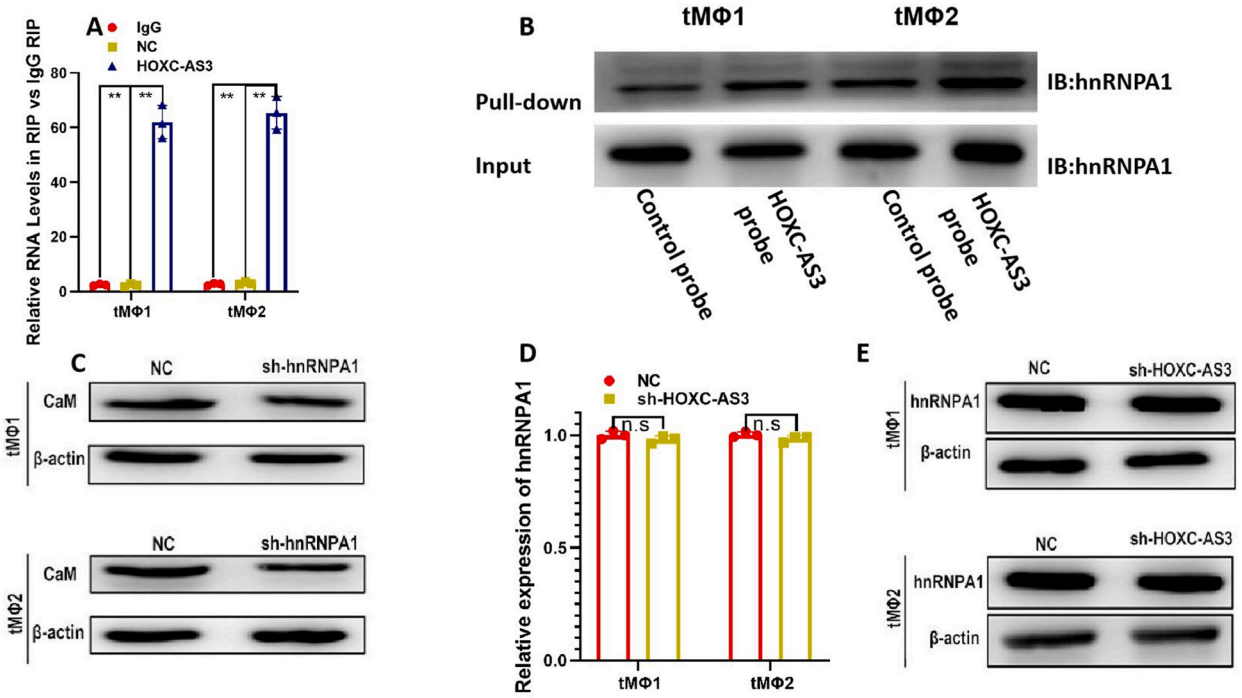

Fig. 5. HOXC-AS3 regulated CaM expression by binding hnRNPA1. **A** RNA pull down assay showed that hnRNPA1 protein was pulled down by the HOXC-AS3 probe. **B** RIP assay showed that HOXC-AS3 was precipitated by the hnRNPA1 antibody in $tM\Phi_1$ and $tM\Phi_2$ cells. **C** Knockdown of hnRNPA1 downregulated CaM expression both in $tM\Phi_1$ and $tM\Phi_2$ cells. **D, E** QRT-PCR and Western blot showed that hnRNPA1 expression did not change significantly at transcription or protein level after HOXC-AS3 knockdown. (**$P < 0.001$, n.s no statistical significance).

phosphorylation, acetylation or ubiquitination) in a variety of lipid metabolism processes, including cholesterol regulatory element binding proteins, thus participating in lipid metabolism regulation [33,34]. Our data supported that HOXC-AS3 can increase lipid metabolism and promote the malignant phenotype in tMΦs by regulating CaM expression.

HnRNPA1 is associated with the development of malignant tumours in various cancer types, such as breast cancer, lung cancer, gastrointestinal cancer, and gliomas [35–37]. The relationship between hnRNPA1 and tumour lipid metabolism has not been explored previously. Our study found that hnRNPA1 can increase lipid metabolism in tMΦs by regulating CaM expression in the GSC microenvironment and that HOXC-AS3 can bind to hnRNPA1. However, HOXC-AS3 expression did not affect hnRNPA1 transcription directly, so hnRNPA1 expression was stable. However, binding of HOXC-AS3 to hnRNPA1 reduced the levels of free hnRNPA1, which can bind with CaM, thus producing a similar effect to that of CaM upregulation.

5. Conclusion

In the current study, we have shown that malignant tMΦs induced by GSC in the GIME exhibited aberrant lipid metabolism. Moreover, lncRNA HOXC-AS3 regulated CaM expression by directly binding with hnRNPA1, leading to lipid metabolism remodelling and promoting the proliferation and invasiveness of tMΦs. Clarifying the role of lipid metabolism remodelling in the GIME will provide an experimental basis for targeted intervention against tMΦs via metabolism regulation and further help to improve the efficacy of GBM immunotherapy. However, our experimental results are mainly based on in vitro and in vivo xenograft models. These preclinical findings may not accurately mimic the complex tumour microenvironment of glioma patients. So high-throughput single-cell molecular sequencing is required to further validate the molecular mechanisms of gene regulatory networks for promising clinical applications.

Ethics approval

This study was performed in line with the principles of the Declaration of Helsinki. Approval was granted by the Ethics Committee of Soochow University (Approval No. SUDA20210708A03, Date: Jul 8, 2021).

Author contribution statement

Yujing Sheng, Baomin Chen, Liu liang: Performed the experiments; Analyzed and interpreted the data; Wrote the paper.
Jun Dong and Zhe Li: Conceived and designed the experiments; Contributed reagents, materials, analysis tools or data.

Suwen Li, Shilu Huang and Shan Cheng: Analyzed and interpreted the data.
Yifang Ping and Zhigang Gong: Contributed reagents, materials, analysis tools or data.

Data availability statement

Data will be made available on request.

Funding statement

This work was supported by National Natural Science Foundation of China (Grant numbers 82203637), Science and Technology Development Foundation of Nanjing Medical University (Grant numbers NMUB20210220), Jiangsu Province Key Research and Development Program: Social Development Project (Grant numbers BE2021653), Natural Science Foundation of Jiangsu Province (Grant numbers BK20201172), Key Program of Health Commission of Jiangsu Province (Grant numbers ZBD2020016) and Suzhou Special Project on Diagnosis and Treatment Technology of Clinical Key Disease (Grant numbers LCZX201915).

Declaration of competing interest

The authors declare that they have no known competing financial interests or personal relationships that could have appeared to influence the work reported in this paper.

Appendix A. Supplementary data

Supplementary data related to this article can be found at https://doi.org/10.1016/j.heliyon.2023.e19034.

References

[1] Q.T. Ostrom, G. Cioffi, H. Gittleman, et al., CBTRUS statistical report: primary brain and central nervous system tumors diagnosed in the United States in 2012-2016, Neuro Oncol. 1 (2019) 21 (Supplement_5): v1-v100.
[2] A.F. Hottinger, A. Ben Aissa, V. Espeli, et al., Phase I study of sorafenib combined with radiation therapy and temozolomide as first-line treatment of high-grade glioma, Br. J. Cancer 118 (6) (2018) e10.
[3] T. Xie, B. Liu, C.G. Dai, Z.H. Lu, J. Dong, Q. Huang, Glioma stem cells reconstruct similar immunoinflammatory microenvironment in different transplant sites and induce malignant transformation of tumor microenvironment cells, J. Cancer Res. Clin. Oncol. 145 (2019) 321–328.
[4] X. Dai, Y. Wang, X. Dong, et al., Downregulation of miRNA-146a-5p promotes malignant transformation of mesenchymal stromal/stem cells by glioma stem-like cells, Aging (Albany NY) 12 (2020) 9151–9172.
[5] H. Wang, H. Li, Q. Jiang, et al., HOTAIRM1 promotes malignant progression of transformed fibroblasts in glioma stem-like cells remodeled microenvironment via regulating miR-133b-3p/TGFβ axis, Front. Oncol. 11 (2021), 603128.
[6] L. Liu, Y. Zhou, X. Dong, et al., HOTAIRM1 maintained the malignant phenotype of tMSCs transformed by GSCs via E2F7 by binding to FUS, JAMA Oncol. 2022 (2022), 7734413.
[7] L.H. Geraldo, Y. Xu, L. Jacob, et al., SLIT2/ROBO signaling in tumor-associated microglia and macrophages drives glioblastoma immunosuppression and vascular dysmorphia, J. Clin. Invest. 131 (16) (2021), e141083.
[8] Z. Zhu, H. Zhang, B. Chen, et al., PD-L1-Mediated immunosuppression in glioblastoma is associated with the infiltration and M2-polarization of tumor-associated macrophages, Front. Immunol. 11 (2020), 588552.
[9] R.S. Andersen, A. Anand, D.S.L. Harwood, B.W. Kristensen, Tumor-associated microglia and macrophages in the glioblastoma microenvironment and their implications for therapy, Cancers 13 (17) (2021) 4255.
[10] N. Tong, Z. He, Y. Ma, et al., Tumor associated macrophages, as the dominant immune cells, are an indispensable target for immunologically cold tumor-glioma therapy? Front. Cell Dev. Biol. 9 (2021), 706286.
[11] R.O. Lu, W.S. Ho, Mitochondrial dysfunction, macrophage, and microglia in brain cancer, Front. Cell Dev. Biol. 8 (2020), 620788.
[12] J. Xu, J. Zhang, Z. Zhang, et al., Hypoxic glioma-derived exosomes promote M2-like macrophage polarization by enhancing autophagy induction, Cell Death Dis. 12 (4) (2021) 373.
[13] A. Wang, X. Dai, B. Cui, et al., Experimental research of host macrophage canceration induced by glioma stem progenitor cells, Mol. Med. Rep. 11 (2015) 2435–2442.
[14] L. Hong, J. Ma, H. Zhu, et al., STAT3 signaling pathway regulates glioma stem cells induced host macrophage malignance, Transl. Cancer Res. 5 (6) (2016) 805–816.
[15] X. Ji, J. Shi, X. Dai, et al., Relevant molecular characteristics analysis on malignant transformation of interstitial cells induced by tumor stem cells in glioma micro-environment, Natl. Med. J. China (Peking) 98 (41) (2018) 3339–3344.
[16] Y. Sheng, Q. Jiang, X. Dong, et al., 3-Bromopyruvate inhibits the malignant phenotype of malignantly transformed macrophages and dendritic cells induced by glioma stem cells in the glioma micro-environment via miR-449a/MCT1, Biomed. Pharmacother. 121 (2020), 109610.
[17] Y. Xiang, H. Miao, Lipid Metabolism in tumor-associated macrophages, Adv. Exp. Med. Biol. 316 (2021) 87–101.
[18] P. Su, Q. Wang, E. Bi, et al., Correction: enhanced lipid accumulation and metabolism are required for the differentiation and activation of tumor-associated macrophages, Cancer Res. 82 (2022) 945.
[19] A. Rafiee, F. Riazi-Rad, M. Havaskary, F. Nuri, Long noncoding RNAs: regulation, function and cancer, Biotechnol. Genet. Eng. Rev. 34 (2) (2018) 153–180.
[20] B. Yang, L. Sun, L. Liang, LncRNA HOXC-AS3 suppresses the formation of mature miR-96 in ovarian cancer cells to promote cell proliferation, Reprod. Sci. 28 (8) (2021) 2342–2349.
[21] S.H. Shi, J. Jiang, W. Zhang, et al., A Novel lncRNA HOXC-AS3 acts as a miR-3922-5p sponge to promote breast cancer metastasis, Cancer Invest. 38 (1) (2020) 1–12.
[22] X. Wang, Y. Sun, T. Xu, et al., HOXB13 promotes proliferation, migration, and invasiveness of glioblastoma through transcriptional upregulation of lncRNA HOXC-AS3, J. Cell. Biochem. 120 (9) (2019) 15527–15537.

[23] Y. Li, L. Peng, X. Cao, et al., The long non-coding RNA HOXC-AS3 promotes glioma progression by sponging miR-216 to regulate F11R expression, Front. Oncol. 12 (2022), 845009.
[24] E.R. Stanley, Murine bone marrow-derived macrophages, Methods Mol. Biol. 75 (1997) 301–304.
[25] K. Kanwore, K. Kanwore, G.K. Adzika, et al., Cancer metabolism: the role of immune cells epigenetic alteration in tumorigenesis, progression, and metastasis of glioma, Front. Immunol. 13 (2022), 831636.
[26] M. Strickland, E.A. Stoll, Metabolic reprogramming in glioma, 5:43, Front. Cell Dev. Biol. 87 (2017) 88.
[27] R.T. Netea-Maier, J.W.A. Smit, M.G. Netea, Metabolic changes in tumor cells and tumor-associated macrophages: a mutual relationship, Cancer Lett. 28 (413) (2018) 102–109.
[28] Y.R. Na, S. Je, S.H. Seok, Metabolic features of macrophages in inflammatory diseases and cancer, 28, Cancer Lett. 413 (2018) 46–58.
[29] J.M. Poczobutt, S. De, V.K. Yadav, et al., Expression profiling of macrophages reveals multiple populations with distinct biological roles in an immunocompetent orthotopic model of lung cancer, J. Immunol. 196 (2016) 2847–2859.
[30] P. Goossens, J. Rodriguez-Vita, A. Etzerodt, et al., Membrane cholesterol effux drives tumor-associated macrophage reprogramming and tumor progression, Cell Metabol. 29 (6) (2019) 1376–1389.e4.
[31] M.F. Tavazoie, I. Pollack, R. Tanqueco, et al., LXR/ApoE activation restricts innate immune suppression in cancer, Cell 172 (4) (2018) 825–840.
[32] Y. Zhang, R. Kurupati, L. Liu, et al., Enhancing $CD8^{+}$T Cell fatty acid catabolism within a metabolically challenging tumor micro-environment increases the efficacy of melanoma immunotherapy, Cancer Cell 32 (3) (2017) 377–391.
[33] J. Wang, W. Yang, Z. Chen, et al., Long noncoding RNA lncSHGL recruits HnRNPA1 to suppress hepatic gluconeogenesis and lipogenesis, Diabetes 67 (4) (2018) 581–593.
[34] Y. Wang, J. Viscarra, S.J. Kim, H.S. Sul, Transcriptional regulation of hepatic lipogenesis, Nat. Rev. Mol. Cell Biol. 16 (11) (2015) 678–689.
[35] R. Roy, Y. Huang, M.J. Seckl, O.E. Pardo, Emerging roles of hnRNPA1 in modulating malignant transformation, Wiley Interdiscip Rev RNA 8 (6) (2017).
[36] W.J. Li, Y.H. He, J.J. Yang, et al., Profiling PRMT methylome reveals roles of hnRNPA1 arginine methylation in RNA splicing and cell growth, Nat. Commun. 12 (1) (2021) 1946.
[37] L. Qiao, Y. Bai, N. Xie, N. Liu, J. Wang, LncRNA ANCR promotes hepatocellular carcinoma metastasis through upregulating hnRNPA1 expression, RNA Biol. 17 (3) (2020) 381–394.